

Communication

HKUST-1-Doped High-Resolution Volume Holographic Gratings

Riccardo Castagna ^{1,2,*} , Alessia Tombesi ³ , Cristiano Riminesi ^{2,*} , Andrea Di Donato ⁴ ,
Oriano Francescangeli ⁵  and Daniele Eugenio Lucchetta ^{5,6,*} 

- ¹ URT-CNR, Università di Camerino (UNICAM), Polo di Chimica, Via Sant'Agostino, 1, 62032 Camerino (MC), Italy
² CNR, Institute of Heritage Science, Via Madonna del Piano, 10, 50019 Sesto Fiorentino (FI), Italy
³ CHIP, Scuola di Farmacia, UNICAM, Via Madonna delle Carceri, 62032 Camerino, Italy
⁴ Dipartimento di Ingegneria dell'Informazione (DII), Università Politecnica delle Marche, Via Brezze Bianche, 60131 Ancona, Italy
⁵ Dipartimento SIMAU, Università Politecnica delle Marche, Via Brezze Bianche, 60131 Ancona, Italy
⁶ Optoacoustic Lab, Dipartimento SIMAU, Università Politecnica delle Marche, Via Brezze Bianche, 60131 Ancona, Italy
* Correspondence: riccardo.castagna@cnr.it (R.C.); cristiano.riminesi@cnr.it (C.R.); d.e.lucchetta@univpm.it (D.E.L.)

Abstract: We report on transmission holographic gratings doped with metal organic frameworks (MOFs). As a first attempt, we focused on MOF-199, also known as HKUST-1, which is an efficient adsorbent of VOCs. HKUST-1 is not soluble in the pre-polymerized holographic mixture. For this reason, samples containing HKUST-1 show high light scattering. In this work, the recording of HKUST-1-doped one-dimensional transmission phase gratings is demonstrated. The optical properties of the recorded structures, such as diffraction efficiency and average refractive index changes, are reported by using angular analysis measurements. A first attempt to demonstrate the possibility of using the doped gratings as sensors is also reported.

Keywords: holography; gratings; metal organic framework; volatile organic compounds; polymers; sensors



Citation: Castagna, R.; Tombesi, A.; Riminesi, C.; Di Donato, A.; Francescangeli, O.; Lucchetta, D.E. HKUST-1-Doped High-Resolution Volume Holographic Gratings. *Chemosensors* **2022**, *10*, 310. <https://doi.org/10.3390/chemosensors10080310>

Academic Editor: Ali Othman

Received: 13 July 2022

Accepted: 3 August 2022

Published: 5 August 2022

Publisher's Note: MDPI stays neutral with regard to jurisdictional claims in published maps and institutional affiliations.



Copyright: © 2022 by the authors. Licensee MDPI, Basel, Switzerland. This article is an open access article distributed under the terms and conditions of the Creative Commons Attribution (CC BY) license (<https://creativecommons.org/licenses/by/4.0/>).

1. Introduction

The ability of metal organic frameworks (MOFs) to adsorb harmful gases is very well known and assessed [1,2]. MOFs allow the adsorption of many kinds of gases, such as SO₂, NH₃, Cl₂, and CO [1]. The adsorptive behavior of MOFs is also studied in the presence of semi-VOCs, volatile fatty acids (VFAs), phenols, and indoles. In particular, the ability of some MOFs to adsorb semi-VOCs with strong affinity towards the polar ones (such as skatole), rather than the non-polar ones (such as benzene), is well established [3]. In these studies, a very strong affinity of HKUST-1, also known as MOF-199, towards polar VOCs is reported. As a matter of fact, HKUST-1 is even suitable for the solid-phase micro-extraction of VOCs from air samples [4]. From an optical point of view, MOFs are studied using the light-matter interactions once guest-VOCs are adsorbed in host-MOFs. The adsorption of the guest-VOCs in the host-MOFs determines changes in the average refractive index of the grating structure that are detected by using optical holography [5,6]. The average grating refractive index changes can be also detected with very high sensitivity by using different optical techniques [7–9]. In this work, angular selectivity measurements are used to detect and characterize MOF-doped holographic gratings (H-MOFs) where the HKUST-1 is the used MOF. Moreover, the same experimental technique is used to detect the presence of VOCs in these MOF-doped holographic gratings. To summarize, in this study, we explore the possibility of incorporating MOFs into a high-resolution transmission grating and use this structure as a high-sensitivity sensor for the detection of VOCs through angular selectivity measurements.

2. Materials and Methods

In this study, 1-vinyl-2-pyrrolidone (NVP), di-pentaerythritol-penta/hexa-acrylate (DPHPA), a couple of photo-initiators, namely bisacylphosphine oxide (I819) and 4,5,6,7-tetrachloro-2',4',5',7'- tetraiodofluorescein (RB), benzene-1,3,5-tricarboxylate (BTC), copper nitrate trihydrate ($\text{Cu}(\text{NO}_3)_2 \cdot 3\text{H}_2\text{O}$), and ethanol (EtOH) came from Merck, Darmstadt, Germany; HKUST-1 was synthesized by us.

2.1. HKUST-1 Synthesis

HKUST-1 was synthesized by us, as previously reported in the literature [10].

2.2. H-MOF₁ Mixture Preparation

The procedure involves the following four steps: (1) HKUST-1 is reduced to a fine powder; (2) 90% *w/w* of DPHPA monomer and 10% *w/w* of HKUST-1 are blended together under magnetic stirring for 24 h to form the MIX-A; separately, (3) NVP 10% *w/w* is mixed with DPHPA 80% and 10% MIX-A are blended together for a further 3 days; (4) finally, 0.1% RB and 0.1% I819 are added. The system is left under stirring for many days in darkness. Then, the system is put to rest at room temperature and under darkness, to allow the deposition of insoluble HKUST-1 on the bottom of the reaction environment. At this step, the HMOF₁ is filtered and a homogeneous suspension is obtained.

Summarizing, the final mixture contains 1% HKUST-1, 0.1% RB, 0.1% I819, 89% DPHPA, 10% NVP.

2.3. H-MOF₂ Mixture Preparation

The mixture is prepared by suspending 3% HKUST-1 in a mixture containing 0.1% RB dispersed in DPHPA. The mixture is kept under magnetic stirring for 1 week. Finally, a droplet of the H-MOF₂ mixture is placed between two microscope glasses.

2.4. Sample Preparation

Samples with two different thicknesses (50 μm and 5 μm) are prepared. The mixture is inserted by capillarity in a sandwich formed by two 1-mm-thick microscope glass slides separated by mylar spacers.).

2.5. Hologram Recording and Optical Characterization Set-Up

In Figure 1a is reported the holographic set-up used to write holograms in reflection geometry. Two CW s-polarized laser beams operating at $\lambda_w = 532$ nm are used to write a one-dimensional (1D) holographic periodic structure in our samples. The irradiated area has a radius of ≈ 2.5 mm, and the writing power is 150 mW per beam. When the 1D interference pattern impinges on the holographic photo-polymerizable material, photo-polymerization and phase separation between the different components of the starting mixture occur [11,12]. The final result is a grating formed by a periodic distribution of inert compound-rich domains, corresponding to the dark regions of the interference pattern, and solid polymer-rich domains corresponding to the illuminated areas of the light spot. The recorded structures are optically characterized by using the setup reported in Figure 1b. In this setup, the sample is placed on a stepper goniometer having an angular resolution of 0.036 degrees and rotates around the Bragg angle corresponding to the red He-Ne wavelength. For each angle, two photo-detectors connected to a data acquisition system acquire the transmitted and diffracted signals.

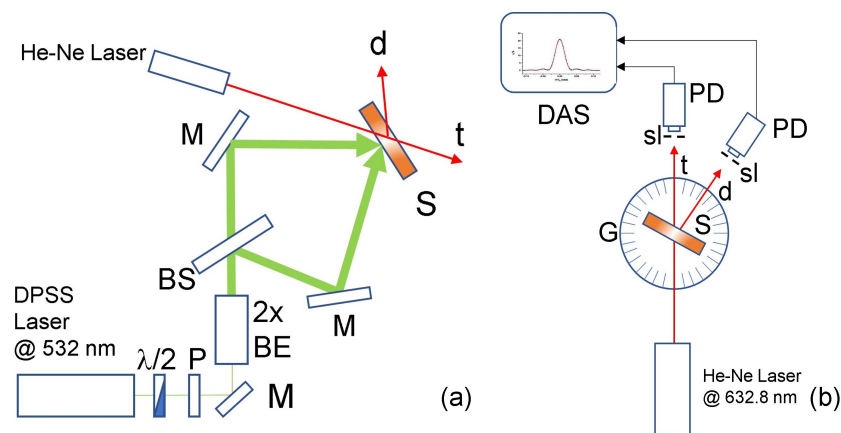


Figure 1. Schematic representation of the writing (a,b) angular analysis set-ups. G = computer-controlled goniometer; $\lambda/2$ = half wavelength plate; P = polarizer; M = mirror; 2x BE = 2x beam expander; BS = beam splitter; S = sample; d and t = diffracted and transmitted beams, respectively; PD = photo-detector; sl = slit; DAS = data acquisition system.

3. Results

Two different mixtures, H-MOF₁ and H-MOF₂, and two different thicknesses (50 and 5 μm) are used in our experiments. Typical samples containing the recorded holograms are reported in Figure 2. After the writing process, the grating area is transparent. Angular selectivity data, acquired with the setup sketched in Figure 1b concerning the two used thicknesses, are reported in Figure 3a and 3b, respectively. In particular, the normalized intensities of the diffracted beams as a function of the difference between the incidence angle and the Bragg angle are reported. By applying the Kogelnik theory, a good agreement between experimental data and theory is obtained and superimposed as a red line in both figures. The calculated diffraction efficiency for the high-resolution transmission grating written in the thick samples is $\approx 0.8\%$, while for the thinner ones, the diffraction efficiency is $\approx 0.1\%$. A different set of measurements concerns H-MOF₂ (see Figure 4). The measured diffraction efficiency for the H-MOF₂-doped samples is higher ($\approx 6\%$) with respect to the ones previously measured in H-MOF₁-doped samples. Due to the better signal to noise ratio, in the following, a first qualitative approach to establish the possibility to use H-MOF₂ as a sensor is reported. To this aim, we used 90% denatured alcohol containing aldehydes and esters derived from the fabrication procedure. The results are summarized in Figure 4. In this figure, the empty circles represent the intensity of the diffracted beam as a function of the angle variations $\Delta\theta = \theta - \theta_B$ after removing one glass slide from the sandwich forming the sample. After 30 min of exposure to alcohol vapors, the angular analysis shows higher diffraction efficiency values, as reported in Figure 4 as a continuous red line. At the end of this process, we heated the sample using a warm-air gun for a few minutes. By repeating the angular analysis, we found the same starting values of diffraction efficiency. In the figure, they are reported as filled triangles. In other words, the sample reverts to its initial state.

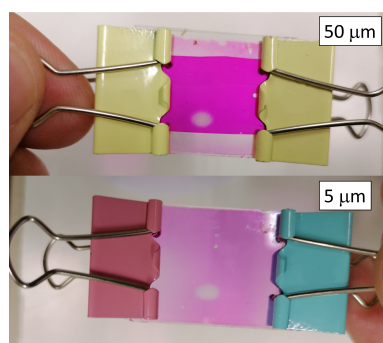


Figure 2. Typical thick and thin samples recorded with the setup reported in Figure 1a.

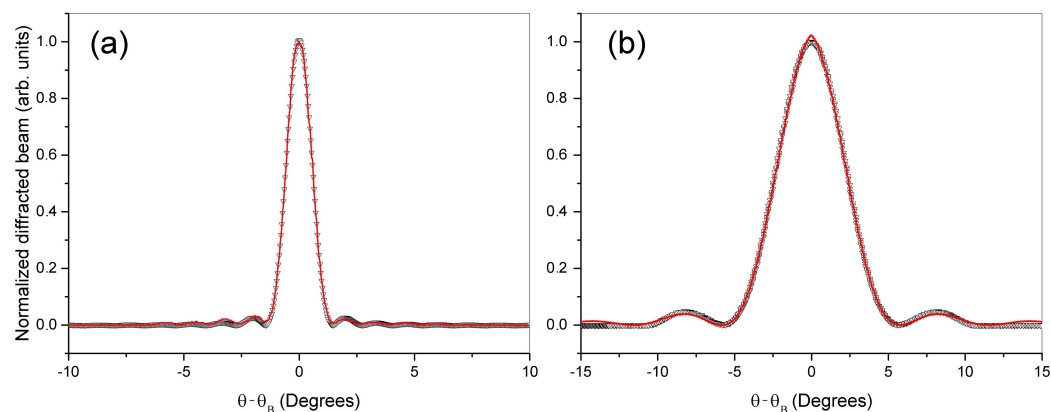


Figure 3. Intensity of the diffracted beam as function of the difference between the incidence angle and the Bragg angle for (a) thick and (b) thin samples. The red curve represents the fit of the experimental data obtained with the Kogelnik theory.

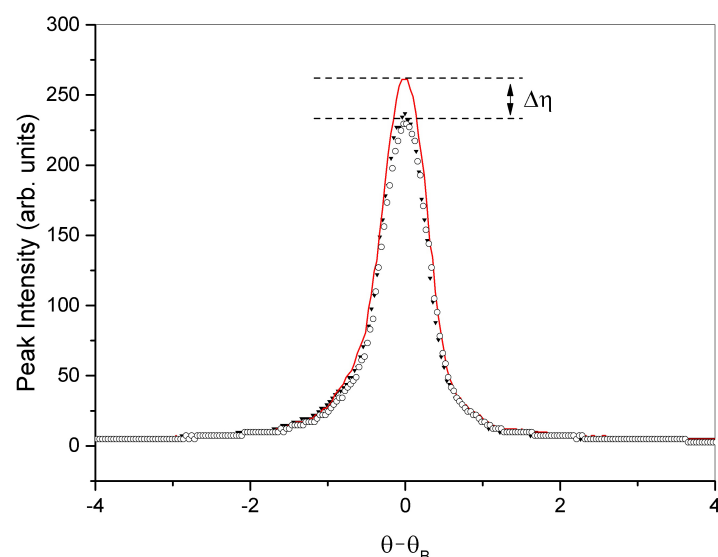


Figure 4. Intensity of the diffracted beam as function of $\Delta\theta = \theta - \theta_B$ after removing one glass slide (empty circles), after 30 min of exposure to denatured 90% alcohol vapors (continuous red line), after heating with a warm-air gun for a few minutes (filled triangles).

4. Discussion

The aim of our work is to demonstrate the feasibility of creating holographic gratings containing MOFs (H-MOFs) where HKUST-1 is the MOF dopant. As specified in the Materials and Methods section, holographic gratings are recorded by using a one-dimensional interference pattern of light at $\lambda = 532$ nm on a photo-polymerizable multi-functional acrylate monomer mixture. This mixture has been used in recent years as a basic mixture for many photonic applications [13,14]. The main physical properties of multi-functional acrylates reside in their ability to store in a high-resolution periodic structure (~ 2000 lines/mm) information related to the incoming polymerizing light, such as polarization [15,16], phase, and wavelength [17]. The main issue in realizing holographic gratings made by acrylate and MOFs resides in the inhomogeneity of the pre-polymerized mixture, because HKUST-1 is not soluble in acrylate. To increase the sensitivity of our gratings, we tried two different approaches: in the first one (H-MOF₁), the sample is fabricated in a low-viscosity environment by adding NVP to the mixture as a cross-linker and solubilizer for DPHPA [18]. Furthermore, in appropriate relative concentrations, NVP is known to increase the photo-polymerization rate in holographic grating systems [19]. In this case, HKUST-1 is deposited on the bottom of the reaction environment and a homogeneous

suspension is easily obtainable by filtration (see Materials and Methods). In the second approach, to increase the sensor's ability in detecting VOCs, we simplified the mixture by using a three-component mixture in which NVP was not present (H-MOF₂). Taking into account H-MOF₁, in order to verify the effects of the sample thickness on the optical properties of the recorded periodic structures, we realized the grating on thick (50 μm) and thin (5 μm) samples. Two typical holograms are shown in Figure 2. At a first visual inspection, the grating spot is transparent, which is a clear signature of the consumption of the photo-initiator under photo-polymerization. The results of the angular analysis related to 50 μm and 5 μm thicknesses are reported in Figures 3a and 3b, respectively. From these plots, it is possible to retrieve the diffraction efficiency of the grating, the grating pitch, and the grating refractive index modulation for each sample. The diffraction efficiency is defined as $\eta = I_i / (I_t + I_d)$, where I_i is the impinging intensity, and I_d and I_t are the diffracted and transmitted intensities, respectively. In our samples, the measured maximum diffraction efficiency values are ~0.8% for the thick ones and ~0.1% for the thin ones. Both values are very low, probably due to the effects of the low concentration of MOF in the suspended H-MOF₁ mixture. In any case, the diffracted beam is still present and detectable by using the high-sensitivity experimental setup reported in Figure 1b. The Full Width at Half Maximum (FWHM) relative to the central peak is approximately ~0.022 and ~0.1 rad for the thick and thin sample, respectively. The well-known expression of the diffraction efficiency, derived by the theory [20], can be used to fit the experimental data. Accordingly, the diffraction efficiency of a one-dimensional transmission phase grating can be written as:

$$\eta(d) = e^{-2\alpha d} \frac{\sin\left(\frac{\sqrt{v^2 + \zeta^2}}{v}\right)^2}{1 + \frac{\zeta^2}{v^2}} \quad (1)$$

with coupling and detuning parameters, respectively, defined as:

$$v = \frac{\pi \delta n d}{\lambda \cos(\theta)} \quad (2)$$

$$\zeta = \Delta\theta \beta d \sin(\theta_B) \quad (3)$$

where δn is the induced refractive index variation, d the grating thickness, λ the reading wavelength in the free space, θ the angle of incidence, θ_B the Bragg angle, $\Delta\theta = \theta - \theta_B$, n the average refractive index of the medium and $\beta = 2\pi n / \lambda$. The agreement between the theoretical expression and the experimental data is excellent and allows the determination of the grating refractive index modulation $\delta n \sim 0.013$ for the thick samples and $\delta n \sim 0.027$ for the thin ones using a measured Bragg angle $\theta_B = 0.448$ rad. The grating thickness derived from the fit of the thick samples gives a value ≈ 20 μm, indicating a partial writing of the grating inside the volume of the sample, due probably to the strong attenuation of the writing light intensity inside the sample itself. In order to check the sensitivity of the H-MOFs in detecting volatile compounds, we tested the grating containing the H-MOF₂, having a higher concentration of HKUST-1. Once the grating was formed and characterized (diffraction efficiency ca. 6%), the sandwich was opened by removing one glass slide. After this, we placed the sample in proximity to a small Petri dish containing 5 mL of denatured alcohol 90% in a sealed environment. In this experimental condition, the grating is exposed—at room temperature—to the vapor alcohol and, reasonably, to aldehydes (keto-aldehydes) and esters, which are the waste products of the food industry from which the denatured alcohol derives. The intensity of the signal increases after 30 min of exposure, as reported in Figure 4, strongly suggesting the adsorption of the volatile compounds present in the denatured alcohol by the MOF. As a counter-proof, we heated the sample for 5 min to a temperature of 100 °C and repeated the measurement. The result, illustrated in Figure 4, indicates the decreases in the intensity of the signal to the starting value, reasonably due to the decrease in the average refractive index between the polymerized and MOF-containing parts. The sample is then left for many hours at room temperature

in aerobic conditions and the angular analysis is repeated, with no observable changes in the diffraction intensity. The series of measurements is repeated several times, reporting substantially the same results. Even if the mixture and the experimental techniques could be improved by adding further tests, these results strongly suggest that H-MOFs are suitable for the highly sensitive detection of VOCs, with possible applications in many contexts (e.g., the detection of VOCs—deriving from the degradation of coatings in paintings and frescos—is very important in heritage science).

5. Conclusions

We obtained gratings with different H-MOF formulations and at different sample thicknesses. While the diffraction efficiency is very low (ca. 0.8% vs. ca. 6%), the angular analysis clearly reports on the grating formation and its quality. By angular analysis, it is also possible to monitor the ability of the H-MOF sensor to detect towards denatured alcohol. A first series of measurements demonstrating the sensor activity is reported.

Author Contributions: Conceptualization, R.C., D.E.L. and C.R.; methodology, R.C., D.E.L. and A.T.; software, A.D.D.; validation, R.C. and D.E.L.; formal analysis, A.D.D.; investigation, R.C. and D.E.L.; resources, R.C. and C.R.; writing—original draft preparation, R.C. and D.E.L.; writing—review and editing, D.E.L., R.C., A.D.D., O.F., A.T. and C.R.; supervision, C.R., O.F. and A.T.; project administration, C.R. and R.C.; funding acquisition, R.C. and C.R. All authors have read and agreed to the published version of the manuscript.

Funding: R.C., A.T. and C.R. thank the Marche Applied Research Laboratory for Innovative Composites (MARLIC), POR Marche FESR 2014–2020, Regione Marche (Italy).

Institutional Review Board Statement: Not applicable.

Informed Consent Statement: Not applicable.

Data Availability Statement: Data are available from the authors under reasonable request.

Acknowledgments: R.C., A.T. and C.R. acknowledge the support of the “Marche Applied Research Laboratory for Innovative Composites” (MARLIC), POR Marche FESR 2014–2020, Regione Marche (Italy). Dedicated to the memory of Temistocle Calzecchi Onesti, the coherer’s inventor, and to Stefano Mircoli, medical pathologist, on the occasion of the hundredth anniversary of their deaths.

Conflicts of Interest: The authors declare no conflict of interest.

References

1. Britt, D.; Tranchemontagne, D.; Yaghi, O.M. Metal-organic frameworks with high capacity and selectivity for harmful gases. *Proc. Natl. Acad. Sci. USA* **2008**, *105*, 11623–11627. [[CrossRef](#)] [[PubMed](#)]
2. Li, Y.; Xiao, A.S.; Zou, B.; Zhang, H.X.; Yan, K.L.; Lin, Y. Advances of metal-organic frameworks for gas sensing. *Polyhedron* **2018**, *154*, 83–97. [[CrossRef](#)]
3. Vellingiri, K.; Szulejko, J.E.; Kumar, P.; Kwon, E.E.; Kim, K.H.; Deep, A.; Boukhvalov, D.W.; Brown, R.J.C. Metal organic frameworks as sorption media for volatile and semi-volatile organic compounds at ambient conditions. *Sci. Rep.* **2016**, *6*, 27813. [[CrossRef](#)] [[PubMed](#)]
4. Omarova, A.; Baizhan, A.; Baimatova, N.; Kenessov, B.; Kazemian, H. New in situ solvothermally synthesized metal-organic framework MOF-199 coating for solid-phase microextraction of volatile organic compounds from air samples. *Microporous Mesoporous Mater.* **2021**, *328*, 111493. [[CrossRef](#)]
5. Keppler, N.C.; Hindricks, K.D.J.; Behrens, P. Large refractive index changes in ZIF-8 thin films of optical quality. *RSC Adv.* **2022**, *12*, 5807–5815. [[CrossRef](#)] [[PubMed](#)]
6. Wu, J.; Zhang, W.; Wang, Y.; Li, B.; Hao, T.; Zheng, Y.; Jiang, L.; Chen, K.; Chiang, K.S. Nanoscale light-matter interactions in metal-organic frameworks cladding optical fibers. *Nanoscale* **2020**, *12*, 9991–10000. [[CrossRef](#)] [[PubMed](#)]
7. Lucchetta, D.E.; Di Donato, A.; Singh, G.; Tombesi, A.; Castagna, R. Optically tunable diffraction efficiency by photo-mobile holographic composite polymer material. *Opt. Mater.* **2021**, *121*, 111612. [[CrossRef](#)]
8. Vita, F.; Lucchetta, D.E.; Castagna, R.; Criante, L.; Simoni, F. Effects of resin addition on holographic polymer dispersed liquid crystals. *J. Opt. A Pure Appl. Opt.* **2009**, *11*, 024021. [[CrossRef](#)]
9. Lucchetta, D.E.; Vita, F.; Francescangeli, D.; Francescangeli, O.; Simoni, F. Optical measurement of flow rate in a microfluidic channel. *Microfluid. Nanofluid.* **2016**, *20*, 9. [[CrossRef](#)]

10. Loera-Serna, S.; Núñez, L.L.; Flores, J.; López-Simeon, R.; Beltrán, H.I. An alkaline one-pot metathesis reaction to give a $[\text{Cu}_3(\text{BTC})_2]$ MOF at r.t., with free Cu coordination sites and enhanced hydrogen uptake properties. *RSC Adv.* **2013**, *3*, 10962–10972. [[CrossRef](#)]
11. Bunning, T.J.; Natarajan, L.V.; Tondiglia, V.P.; Sutherland, R.L. Holographic Polymer-Dispersed Liquid Crystals (H-PDLCs). *Annu. Rev. Mater. Sci.* **2000**, *30*, 83–115. [[CrossRef](#)]
12. Sutherland, R.L.; Natarajan, L.V.; Tondiglia, V.P.; Bunning, T.J. Bragg gratings in an acrylate polymer consisting of periodic polymer-dispersed liquid-crystal planes. *Chem. Mater.* **1993**, *5*, 1533–1538. [[CrossRef](#)]
13. Castagna, R.; Nucara, L.; Simoni, F.; Greci, L.; Rippa, M.; Petti, L.; Lucchetta, D.E. An Unconventional Approach to Photomobile Composite Polymer Films. *Adv. Mater.* **2017**, *29*, 1604800. [[CrossRef](#)] [[PubMed](#)]
14. Castagna, R.; Lucchetta, D.E.; Rippa, M.; Xu, J.H.; Donato, A.D. Near-frequency photons Y-splitter. *Appl. Mater. Today* **2020**, *19*, 100636. [[CrossRef](#)]
15. Shalit, A.; Lucchetta, D.E.; Criante, L.; Vita, F.; Tasseva, J.R.; Simoni, F.; Franco, L.; Bizzarri, R.; Faraci, P.; Conte, R.; et al. Laser light polarization plastic visualizer: Light scattering distribution and anisotropy. *RSC Adv.* **2013**, *3*, 7677–7680. [[CrossRef](#)]
16. Shalit, A.; Lucchetta, D.; Piazza, V.; Simoni, F.; Bizzarri, R.; Castagna, R. Polarization-dependent laser-light structured directionality with polymer composite materials. *Mater. Lett.* **2012**, *81*, 232–234. [[CrossRef](#)]
17. Castagna, R.; Donato, A.D.; Nucara, L.; Xu, J.H.; Lucchetta, D.E.; Simoni, F. Structured beam diffraction. *Opt. Lett.* **2016**, *41*, 1462–1465. [[CrossRef](#)] [[PubMed](#)]
18. White, T.J.; Liechty, W.B.; Guymon, C.A. The influence of N-vinyl pyrrolidone on polymerization kinetics and thermo-mechanical properties of crosslinked acrylate polymers. *J. Polym. Sci. Part A Polym. Chem.* **2007**, *45*, 4062–4073. [[CrossRef](#)]
19. White, T.J.; Liechty, W.B.; Guymon, C.A. Copolymerization of N-Vinyl Pyrrolidinone with Multifunctional Acrylates. In Proceedings of the RadTech e/5 Technical Proceedings, Chicago, IL, USA, 24–26 April 2006.
20. Kogelnik, H. Coupled wave theory for thick hologram gratings. In *Landmark Papers On Photorefractive Nonlinear Optics*; World Scientific: Singapore, 1995; pp. 133–171.